have obtained ratios of narrow-band images of Venus at 2.24 and 2.4 μm that show small, spatially dependent contrast variations, but their analyses of these images indicates that H_2O variations are much smaller than those seen here, and they are not well correlated with either feature brightness or latitude. The spatially resolved spectra collected by the Galileo NIMS experiment could help to determine the spatial relationship of the NIR features and the trace gas abundances in the lower Venus atmosphere.

The apparent presence of spatially varying H_2O abundances below the clouds has a variety of implications for studies of the deep Venus atmosphere. For example, the spatial distribution of wet and dry regions must be known to estimate the total water budget of the lower Venus atmosphere. The water budget, in turn, affects the efficiency of the atmospheric greenhouse mechanism that maintains the high surface temperatures. Both water vapor and clouds play an important role in this greenhouse by blocking thermal emission in spectral windows between CO_2 bands (*26*). Abundances of H_2O as large as those inferred from our hot-spot spectra, along with an unbroken cloud deck as thick as that used for our cold-spot model are assumed in current greenhouse models to yield the observed surface temperatures (730 K). Thus other greenhouse absorbers or other radiative processes that are not currently included in those models may be needed to account for these high temperatures in consideration of the lower water abundances of cold-spot regions and the lower cloud abundances of hot-spot regions that we have observed.

REFERENCES AND NOTES

1. D. A. Allen and J. W. Crawford, *Nature* **307**, 222 (1984).
2. D. A. Allen, *Icarus* **69**, 221 (1987).
3. L. W. Kamp, F. W. Taylor, S. B. Calcutt, *Nature* **336**, 360 (1988).
4. D. Crisp *et al.*, *Science* **246**, 506 (1989).
5. A. P. Ingersoll *et al.*, *Adv. Space Res.* **7**, 343 (1987); D. Crisp, A. P. Ingersoll, C. E. Hildebrand, R. A. Preston, *ibid.* **10**, 109 (1990).
6. B. Bezard, C. DeBergh, D. Crisp, J.-P. Maillard, *Nature* **345**, 508 (1990).
7. J. H. Hoffman, R. R. Hodges, T. M. Donahue, M. B. McElroy, *J. Geophys. Res.* **85**, 7882 (1980); V. I. Oyama *et al.*, *ibid.*, p. 7891.
8. A. Tokunaga, L. Bergknut, K. Sellgren, *The Cooled Grating Array Spectrometer User's Manual* (NASA Infrared Telescope Facility, Mauna Kea, HI, 1990).
9. This full-aperture (3.0-m) mask had a 1.22-m circular hole that was placed off center, between the telescope's secondary mirror supports, to produce a completely unobstructed aperture. The mask reduced the light collection area of the IRTF by a factor of 6, but this was not a problem because the night side of Venus is relatively bright (visual magnitude ≈ 7). The unobstructed aperture also reduced the amount of light that could be scattered from the bright sunlit crescent onto the night side by eliminating the diffraction from the telescope's secondary mirror support structure.
10. W. M. Sinton, P. Kalas, K.-L. Hodapp, R. Wainscoat, B. Ragent, D. Crisp, *Bull. Am. Astron. Soc.* **22**, 1053 (1990); D. Crisp *et al.*, *ibid.*, p. 1053.
11. J. H. Park *et al.*, *NASA Ref. Publ. 1188* (1987); L. S. Rothman *et al.*, *Appl. Opt.* **26**, 4058 (1987). It should also be noted that the high-temperature CO_2 spectrum is poorly known in the NIR at this time.
12. J. F. Bell III, "Venus CGAS Data Reduction" (Hawaii Institute of Geophysics Internal Report, Honolulu, 1990).
13. K. F. Palmer and D. Williams, *Appl. Opt.* **14**, 208 (1975).
14. The presence of water vapor in Earth's atmosphere impairs studies of water vapor at levels above 1 bar in the Venus atmosphere because the Venus water lines are strongly blended with their much stronger telluric counterparts. The H_2O in the deep atmosphere of Venus produces much larger effects on emission spectra because the pressure-broadened far wings of water lines that are formed at pressures greater than 1 bar are not hidden by their telluric counterparts.
15. D. Crisp, *J. Geophys. Res.* **95**, 14577 (1990).
16. M. Fukabori, T. Nakazawa, M. Tanaka, *J. Spect. Quan. Rad. Trans.* **36**, 265 (1986); *ibid.*, p. 283.
17. M. E. Thomas and R. J. Nordstrom, *Appl. Opt.* **24**, 3526 (1985).
18. J. F. Moore, *NASA–Goddard Space Flight Center Rep. X-630-72-48* (1971).
19. D. Crisp, *Icarus* **67**, 484 (1986).
20. R. G. Knollenberg and D. M. Hunten, *J. Geophys. Res.* **85**, 8039 (1980).
21. A. Seiff *et al.*, *ibid.*, p. 7903.
22. V. I. Moroz, in *Venus*, D. M. Hunten, L. Colin, T. M. Donahue, V. I. Moroz, Eds. (Univ. of Arizona Press, Tucson, 1983), pp. 45–68.
23. This choice was motivated by a comparison between the Pioneer Venus and VEGA entry probe cloud-particle spectrometer measurements. The VEGA lander saw many fewer large particles than the Pioneer Venus large probe (*20*) in the middle and lower clouds [B. E. Moshkin *et al.*, *Sov. Astron. Lett.* **12**, 36 (1986)].
24. The enhanced SO_3 abundance predicted by this scheme cannot be tested because the absorption by SO_3 is not well documented at these wavelengths. Also, this data set alone cannot be used to test the apparent relation between H_2O and cloud amount because all of our 2.3-μm spectra were taken from the same hot and cold spots.
25. D. Crisp *et al.*, in preparation.
26. J. B. Pollack, O. B. Toon, R. Boese, *J. Geophys. Res.* **85**, 8223 (1985).

27. We thank C. Lindsey for the use of his Solar filter mask (which became our Venus mask) and telescope operators B. Golisch and G. Koenig, as well as the rest of the day crew and support scientists of the Infrared Telescope Facility, for their assistance. We also thank A. Tokunaga and T. Brooke for invaluable assistance with CGAS data reduction software. W.M.S. is indebted to K.-L. Hodapp and J. Rayner and their infrared array engineers and technicians and B. Ragent, R. Wainscoat, S. Ridgway, and P. Kalas, who collaborated in making the imaging observations. This work was supported by grants from the NASA Planetary Astronomy and Planetary Atmospheres program to the Jet Propulsion Laboratory, California Institute of Technology, and the University of Hawaii. University of Hawaii Planetary Geosciences Division Publication #645.

17 January 1991; accepted 3 April 1991

Identification of the DNA Binding Site for NGFI-B by Genetic Selection in Yeast

THOMAS E. WILSON, TIMOTHY J. FAHRNER, MARK JOHNSTON, JEFFREY MILBRANDT*

An in vivo selection system for isolating targets of DNA binding proteins in yeast was developed and used to identify the DNA binding site for the NGFI-B protein, a member of the steroid–thyroid hormone receptor superfamily. The feasibility of the technique was verified by selecting DNA fragments that contained binding sites for GCN4, a well-characterized yeast transcriptional activator. The DNA binding domain of NGFI-B, expressed as part of a LexA–NGFI-B–GAL4 chimeric activator, was then used to isolate a rat genomic DNA fragment that contained an NGFI-B binding site. The NGFI-B response element (NBRE) is similar to but functionally distinct from elements recognized by the estrogen and thyroid hormone receptors and the hormone receptor–like proteins COUP-TF, CF1, and H-2RIIBP. Cotransfection experiments in mammalian cells demonstrated that NGFI-B can activate transcription from the NBRE with or without its putative ligand binding domain.

EXPRESSION OF EARLY RESPONSE genes is rapidly and transiently induced in response to various stimuli, including growth factors. These genes often encode transcriptional regulatory proteins [for example *c-fos* and *c-jun* (*1*)] and are thought to activate or repress genes appropriate to the changing cellular environment or to the newly differentiated state. However, the target genes of most mammalian early response genes have not been identified, so their specific functions in cellular differentiation are unknown.

NGFI-B is an early response gene that is induced by nerve growth factor (NGF) in the rat pheochromocytoma cell line PC12 (*2*, *3*). This neural crest-derived cell line responds to NGF by differentiating into a postmitotic cell type with neuronal characteristics (*4*). Sequence analysis shows that NGFI-B shares similarity with the steroid–

T. E. Wilson, T. J. Fahrner, J. Milbrandt, Division of Laboratory Medicine, Departments of Pathology and Internal Medicine, Washington University School of Medicine, St. Louis, MO 63110.
M. Johnston, Department of Genetics, Washington University School of Medicine, St. Louis, MO 63110.

*To whom correspondence should be addressed.

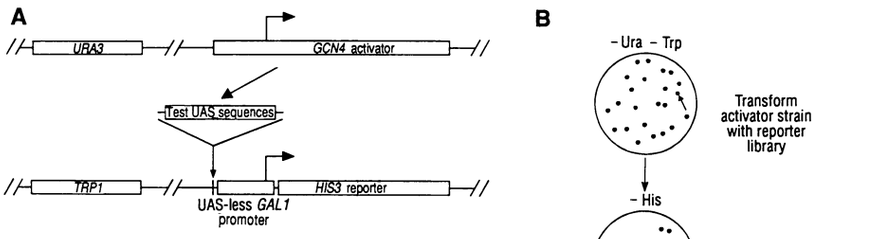

C

	Number obtained	Sequence
GCN4 site		TGACTCA
Random oligonucleotide library selected clones	2	TGACTCA
Rat genomic library selected clones	6	TGACTCA
	1	TGtCTCA
	1	TGgCTCA
	1	TGACTtA
	1	No GCN4 site

Fig. 1. The yeast selection system. (**A**) Schematic of the yeast activator and reporter plasmids. In this example, the activator is GCN4 expressed from its own promoter. (**B**) Selection of yeast bearing specifically activated UAS-reporter clones. An activator-dependent His^+ colony (indicated by the arrow) is identified by the sensitivity of its His^+ phenotype to 5-FOA (that is, it will only grow on plates lacking 5-FOA). (**C**) Three thousand clones from each of the degenerate oligonucleotide and genomic fragment libraries were screened for activation by plasmid-borne *GCN4* in a *gcn4*$^-$ strain [*Saccharomyces cerevisiae* YM3040 (*a ura3-52 his3-200 ade2-101 lys2-801 trp1-501 leu2*$^-$ *trp1*$^-$ *gcn4Δ1*)] (*10*). Two oligonucleotide clones that contained perfect GCN4 consensus sites were independently selected ($P = 2 \times 10^{-4}$) (*31*). Of ten clones isolated from the genomic library, six contained perfect GCN4 sites ($P = 4 \times 10^{-6}$) (*31*) and three contained sites that match the GCN4 binding site at six of the seven base pairs (nonmatching bases are lowercase and underlined). One of the selected fragments had no apparent GCN4 site. All sequences with one or no differences from the GCN4 site are shown.

thyroid hormone receptor superfamily (*2*), a class of ligand-dependent transcriptional activator proteins (*5*). As a potential ligand-dependent transcription factor, the synthesis of which is induced by extracellular signals, NGFI-B might function in NGF-induced neuronal differentiation.

Steroid–thyroid hormone receptors bind to DNA as dimers by virtue of two Cys_2-Cys_2 zinc fingers (*5, 6*). The amino acid sequence of the NGFI-B zinc fingers suggests that the protein might bind to the estrogen (ERE) or thyroid hormone receptor (TRE) response elements (7). However, we have been unable to detect binding of NGFI-B to either of these sites (*8*). To define the DNA binding specificity of the NGFI-B protein, we developed a genetic selection system in yeast that identifies target sequences of DNA binding proteins.

The yeast selection system makes use of two plasmids (Fig. 1A). First, the coding sequence of the *HIS3* gene was placed downstream of an inactive *GAL1* promoter (*9*). This promoter becomes active and expresses *HIS3* only when the binding site of a transcriptional activator protein (upstream activating sequence, or UAS) is inserted upstream. Second, the transcriptional activator gene was present on a plasmid with *URA3* as the selectable marker. A yeast cell that carries this transcriptional activator plasmid and a reporter clone that bears binding sites for the activator protein will express *HIS3* and become His^+. However, with a library of reporter clones, most yeast cells will be His^+ as a result of activation by an endogenous yeast activator, whereas relatively few will be His^+ as a result of activation by the plasmid-borne activator. These possibilities can be distinguished by replica plating to medium containing 5-fluoro-orotic acid (5-FOA) (*10*), which is metabolized to a toxic product by the *URA3* product (*11*). Yeast transformants that require the plasmid-borne activator for function of the test UAS will be His^+ only in the absence of 5-FOA (that is, only when they contain the activator plasmid) (Fig. 1B).

To test the feasibility of the yeast selection system we used the yeast transcriptional activator GCN4, which recognizes the 7-bp consensus sequence TGACTCA (*12, 13*). Two target reporter libraries were created that contained either oligonucleotides of random sequence or rat genomic DNA fragments as potential UASs (*14*). A total of 12 clones that required plasmid-borne *GCN4* in order to be His^+ were selected from these libraries (*10*), and all but one of these contained an apparent GCN4 binding site (Fig. 1C). The selected genomic fragments may be of further interest because the GCN4 recognition site, TGACTCA, is the same as that for the mammalian transcription factor AP-1 (*1, 15*).

A potential limitation of the described selection system is that the DNA binding protein under study must activate transcription in yeast. To surmount this problem, we exploited the LexA-GAL4 hybrid protein (LG), which binds to genes in yeast that contain the LexA binding site (lexO), by virtue of its LexA DNA binding domain, and activates transcription by virtue of its GAL4 transcriptional activating domain (Fig. 2A) (*16*). Because of the apparent modular structure of transcription factors (*17*), addition of another DNA binding domain (X) to LG to create a tripartite protein (LXG) should allow for the transcriptional activation of a reporter gene that contains a binding site for the added domain. Leaving the LexA DNA binding domain intact in the chimera provides an internal control for activator expression and function. The LexA domain should not interfere significantly with selection because its binding site is relatively large (20 bp) (*18*) and should thus occur rarely.

We constructed a chimeric activator by inserting the NGFI-B zinc finger region into LG (*19*). This LexA–NGFI-B–GAL4 (LBG) chimera still activated transcription from a lexO-containing reporter gene, demonstrating that the hybrid activator protein was expressed and functional in yeast cells (Fig. 2A). LBG was then used as the activa-

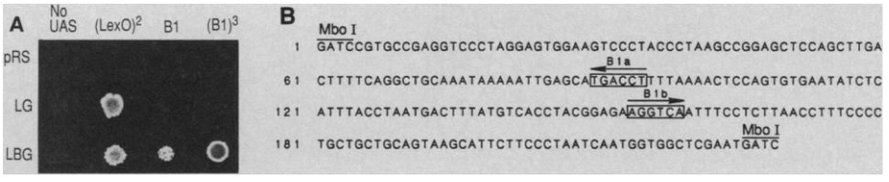

Fig. 2. Selection with a LexA–NGFI-B–GAL4 (LBG) chimera. (**A**) The LBG chimeric activator was used to select a His^+, 5-FOA–sensitive clone (B1) from the genomic fragment reporter library (*10*). Yeast bearing the indicated (at left) activator plasmids were transformed with reporters (indicated at the top) that contained no UAS, two LexA binding sites, or one or three copies of the B1 genomic fragment (*9*), and added to medium that lacked histidine to assess *HIS3* gene expression. The pRS vector is plasmid alone, without added activator protein sequences. The yeast strain was *S. cerevisiae* YM954 (*a ura3-52 his3-200 ade2-101 lys2-801 leu2*$^-$ *trp1-901* can^R *gal4Δ512 gal80Δ338*). (**B**) Sequence of the B1 genomic fragment. The locations of the B1a and B1b sequences are indicated, with boxes surrounding the ERE-TRE half-sites. Relative orientation of the half-sites are indicated by arrows.

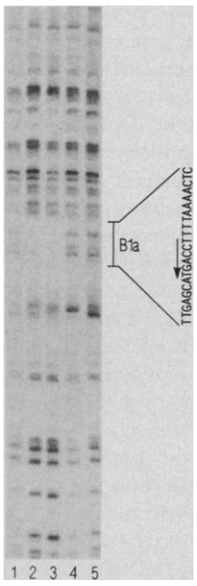

Fig. 3. DNase I footprinting of the B1 genomic fragment with NGFI-B. (Lane 1) The DNase I digestion pattern of the ^{32}P-labeled B1 genomic fragment in the absence of added protein. Regions bound by NGFI-B were detected by first incubating with 15 μg (lanes 2 and 4) or 45 μg (lanes 3 and 5) of an NGFI-B–containing (hsB-CHO) (lanes 2 and 3) or negative control (hs-CHO) (lanes 4 and 5) whole cell extract. The B1a protected region is indicated by a bracket. Sequence location was determined by comparison to an adjacent dideoxy sequencing ladder. Protection assays were performed (*21*) and whole cell extracts were prepared (*32*) essentially as described.

tor in a selection of 60,000 clones of the genomic fragment reporter library (*10*). Two clones that required LBG for *HIS3* expression were identified and shown to be identical. Activation of *HIS3* in one clone (B1) clearly required the NGFI-B zinc fingers because LG-containing yeast cells transformed with this clone were His$^-$ (Fig. 2A). Multiple copies of the B1 genomic fragment inserted upstream of *HIS3* enhanced the LBG-dependent His$^+$ phenotype, further demonstrating the specificity of the interaction (Fig. 2A).

The 229-bp B1 genomic fragment contained two copies of the ERE-TRE half-site, AGGTCA (termed B1a and B1b in Fig. 2B), separated by 58 nucleotides. Inverted repeats of this 6-bp sequence are present in the ERE and TRE, with half-sites juxtaposed in the TRE but separated by three nucleotides in the ERE (*6*). We hypothesized that one or both of these regions would be binding sites for NGFI-B. To test this hypothesis, we performed deoxyribonuclease I (DNase I) footprinting analysis on the B1 fragment (Fig. 3) with a whole cell extract of a cell line (hsB-CHO) that produces large amounts of NGFI-B protein in response to heat shock (*3*). The B1a region was protected by the hsB-CHO cell extract, but not by a control CHO cell extract (hs-CHO). The B1b region was partially protected at high concentrations of hsB-CHO extract (*8*), suggesting that NGFI-B binds to this site with lower affinity.

To assess the difference in affinities of the B1a and B1b sites for NGFI-B, we tested the ability of various concentrations of unlabeled B1a and B1b oligonucleotides to compete for binding of NGFI-B to labeled B1a in a gel retardation assay (Fig. 4A). Consistent with the footprinting results, NGFI-B had a higher affinity for the B1a sequence—approximately three times more B1b than B1a oligonucleotide was required for the same amount of competition.

Because the B1a and B1b oligonucleotides both contain ERE-TRE half-sites but have different affinities for NGFI-B, we reasoned that nucleotides adjacent to the half-sites must also be important for binding. To identify these nucleotides, we used B1a oligonucleotides with sequential mutations to compete for binding of NGFI-B to B1a (Fig. 4). Changes in either the half-site or the AAA sequence immediately 5′ to the half-site effectively eliminated competition. This localized the high affinity B1a NBRE to the ERE-TRE half-site and its three adjacent 5′ A nucleotides. The lower affinity B1b site contained the sequence AGA immediately 5′ to the ERE-TRE half-site, suggesting that one substitution in this region can reduce binding affinity. This mutational analysis argues against the necessity for short-range symmetry in the NGFI-B response element (NBRE) and suggests that dimerization may not be strictly required for NGFI-B to bind to its recognition element, high binding affinity being achieved by extension of the recognition sequence.

To assess whether NGFI-B can bind to the recognition sites of other steroid hormone receptors, we tested several known response elements, all of which contain at least one ERE-TRE half-site, as competitors of NGFI-B binding to B1a (Fig. 4B). Neither the ERE nor TRE inhibited formation of the NGFI-B–B1a complex, even at a 100-fold molar excess. The site for the H-2 region II binding protein (H-2RIIBP), a highly related member of the steroid–thyroid hormone receptor family that binds to major histocompatibility complex class I genes (*20*), was also an ineffective inhibitor of complex formation. By contrast, sites for *Drosophila* chorion factor 1 (CF1) (*21*) and chicken ovalbumin upstream promoter transcription factor (COUP-TF) (*22*) interfered with NGFI-B binding to B1a.

A search of the EMBL sequence database revealed genes that contain the NBRE (defined for this purpose as 5′-AAAAGGTCA, with up to one mismatch in the three 5′ A nucleotides) in their promoter regions. Most notably, genes for the steroid biosyn-

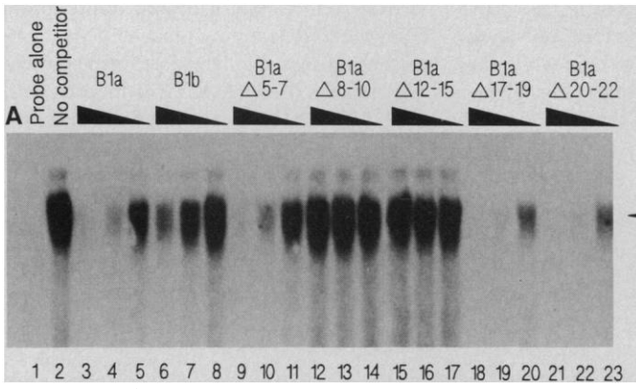

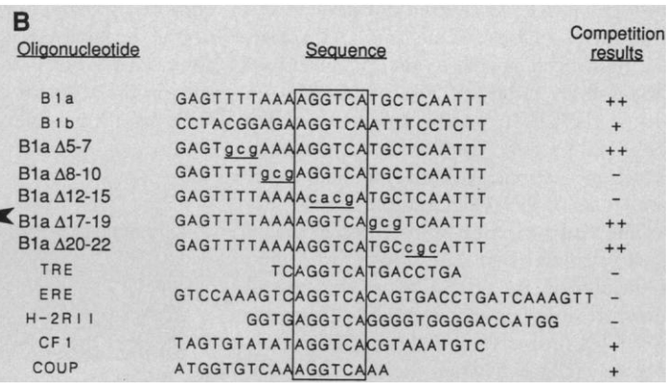

Fig. 4. Definition of the NGFI-B recognition sequence. (**A**) A gel shift assay was performed as described (*21*) with 5 μg of hsB-CHO whole cell extract and double-stranded B1a oligonucleotide labeled with [γ-^{32}P]ATP (adenosine triphosphate) to a specific activity of 10^8 cpm/μg (lane 2). The NGFI-B–B1a complex is indicated by an arrowhead (the free probe was allowed to run off the gel; lane 1, probe alone). For competition, the extract was incubated with 100-fold (lanes 3, 6, 9, 12, 15, 18, 21), 30-fold (lanes 4, 7, 10, 13, 16, 19, 22), and tenfold (lanes 5, 8, 11, 14, 17, 20, 23) molar excesses of the indicated oligonucleotides. (**B**) Summary of gel shift results. The names of the mutant oligonucleotides are derived from the nucleotide numbers of the B1a oligonucleotides that were substituted. Mutated nucleotides are shown in lower case and underlined. The box surrounds the ERE-TRE half-site present in all oligonucleotides except the B1a Δ12-15 mutation. The results of competition of the NGFI-B–B1a gel shift with each oligonucleotide are shown to the right, with ++, +, and − referring to complete, partial, and no competition at a 100-fold molar excess, respectively.

thetic enzymes 21-hydroxylase and cholesterol desmolase and the gene that encodes corticotropin-releasing factor have NBRE sites (*23*). A second group of NBRE-containing genes encodes lipid binding proteins (*24*). Neuron-related NBRE-containing genes include the γ subunit of NGF, the γ subunit of the muscle acetylcholine receptor, and N-*myc* (*25*). Whether or not NGFI-B actually participates in the regulation of these or other NBRE-containing genes remains to be shown.

To assess whether the NBRE could direct NGFI-B–dependent transcriptional activation, we placed the B1 fragment upstream of a basally inactive prolactin promoter–luciferase gene construct and cotransfected the resulting plasmid into COS cells with various NGFI-B–expressing plasmids (*26, 27*) (Fig. 5A). A truncated form of NGFI-B that lacked the putative ligand binding domain (NGFI-Bt) activated transcription ninefold from the B1-luciferase reporter. This result is consistent with observations that similarly truncated glucocorticoid, estrogen, and progesterone receptors activate transcription in the absence of ligand, albeit with reduced efficiency (*28*). Full-length NGFI-B activated luciferase expression from the B1-luciferase reporter to an even greater extent (15-fold) (Fig. 5A). The B1a oligonucleotide also directed dose-dependent, specific activation by cotransfected NGFI-B, as high as 67-fold when multiple copies were present (Fig. 5B), even though no presumptive NGFI-B ligands were added.

There are several possible explanations for the apparent ligand-independent transcriptional activation by NGFI-B: (i) the ligand for NGFI-B may be present in the medium used for growth and transfection of the COS cells; (ii) the ligand for NGFI-B may be an intracellular molecule that is synthesized in COS cells; (iii) NGFI-B may not require a ligand to activate transcription, despite its sequence similarity to other ligand-dependent receptors; and (iv) the extent of activation seen may be weak compared to the amount that would be observed if ligand was added at the appropriate concentration.

Our in vivo binding site selection method has some advantages over in vitro selection procedures (*12, 29*). First, high affinity antibodies, purified protein, and efficient bacterial expression systems are not necessary for application of this procedure. The only tools needed are existing yeast expression plasmids. Thus, after a putative DNA binding protein has been identified, it can immediately be used to select target fragments. Furthermore, use of an LXG tripartite activator protein should allow for determination of binding sequences for any DNA binding protein, even when only the DNA binding domain has been cloned. In addition to the NGFI-B zinc fingers, we have created functional proteins with the GCN4 leucine zipper domain and the NGFI-A zinc fingers (*8*).

Another advantage of the yeast-based method is that selection is performed in vivo and thus may detect more biologically relevant interactions. Because in vitro techniques must be performed under conditions of high stringency to identify specifically bound sites, the examined sites may not reflect the true diversity of DNA binding possible by a given protein. In vivo selection assesses clones individually, and so weaker but functional target clones might also be isolated. This is demonstrated by comparing the GCN4 sites obtained here (Fig. 1C) with those obtained with an in vitro procedure (*12*). In the latter case, 95% of the isolated sites contained a perfect 7-bp GCN4 core consensus sequence. Also, a significant consensus was obtained up to three nucleotides outside of the 7-bp core, despite the fact that many proposed yeast GCN4 target sequences diverge from this added consensus (*13*). In the work presented here, no consensus was seen outside of the 7-bp core, and 33% of the selected clones did not have the perfect 7-bp core; yet all clones required GCN4 for activation, suggesting that biological function does not strictly require a perfect 7-bp binding site, an observation consistent with previous reports (*13*).

There are two disadvantages of the in vivo selection technique. First, the technique cannot be used for proteins that have a DNA binding specificity that is identical to a transcriptional activator present in yeast. Second, fewer test sequences can be screened compared with in vitro techniques, so that an entire mammalian genome cannot be analyzed. However, the smaller genomes of yeast and *Drosophila* can be completely screened (*30*). We therefore suggest that in vitro and in vivo techniques might be used most efficiently in combination. A large target population could be screened by in vitro selection at low stringency. The resulting population would be enriched for both weak and strong target sites (necessarily containing some false positives) and would thus be accessible to screening in yeast. In this way, many weak and strong target sequences could be selected from a mammalian genome, increasing the likelihood of identifying genes that are naturally regulated by a transcription factor.

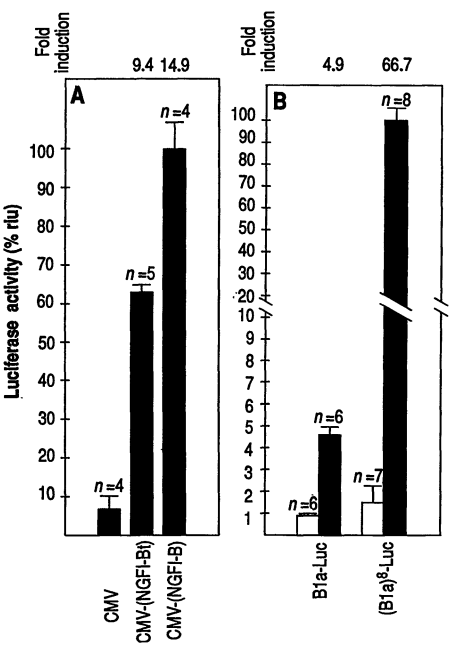

Fig. 5. Transcriptional activation by NGFI-B in mammalian cells. (**A**) Activation of the B1 fragment–containing luciferase reporter (B1-Luc) by various forms of NGFI-B. No luciferase activity was detected when pCMV–(NGFI-B) was cotransfected with the nonrecombinant Pro36-Luc vector. Data were normalized between experiments by expressing values as a percentage of the relative luciferase units (rlu) obtained with the B1-Luc–NGFI-B combination. Fold induction is calculated relative to the B1-Luc–CMV combination. (**B**) Dose-dependent activation of the B1a oligonucleotide–containing reporters [B1a-Luc and $(B1a)^8$-Luc] by NGFI-B. White bars, activation by the nonrecombinant pCMV vector; black bars, activation by pCMV–(NGFI-B). Data were normalized between experiments by expressing values relative to the $(B1a)^8$-Luc–NGFI-B combination. Fold induction for each reporter by NGFI-B is calculated relative to the activity obtained with pCMV. The number of plates assayed for each combination (*n*) is shown above the error bars (SD).

REFERENCES AND NOTES

1. F. J. Rauscher III, L. C. Sambucetti, T. Curran, R. J. Distel, B. M. Spiegelman, *Cell* **52**, 471 (1988); D. Bohmann *et al.*, *Science* **238**, 1386 (1987).
2. J. Milbrandt, *Neuron* **1**, 183 (1988); M. A. Watson and J. Milbrandt, *Mol. Cell. Biol.* **9**, 4213 (1989).
3. T. J. Fahrner, S. L. Carroll, J. Milbrandt, *Mol. Cell. Biol.* **10**, 6454 (1990).
4. L. A. Greene and A. S. Tischler, *Adv. Cell. Neurobiol.* **3**, 373 (1982).
5. R. M. Evans, *Science* **240**, 889 (1988); M. Beato, *Cell* **56**, 335 (1989).
6. C. K. Glass, J. M. Holloway, O. V. Devary, M. G. Rosenfeld, *Cell* **54**, 321 (1988); V. Kumar and P. Chambon, *ibid.* **55**, 145 (1988).
7. K. Umesono and R. M. Evans, *ibid.* **57**, 1139 (1989).
8. T. E. Wilson, T. J. Fahrner, M. Johnston, J. Milbrandt, unpublished data.
9. The basally inactive *HIS3* reporter plasmid was obtained as follows: An Eco RI–Sal I fragment from p1OGH [Y. Lorch and R. D. Kornberg, *J. Mol. Biol.* **186**, 821 (1985)] that contained the *HIS3* coding region and a minimal *GAL1* promoter (lacking a UAS) was cloned into the *URA3-CEN3-ARS1* vector YCP50. The mp7 polylinker was cloned into the Eco RI site upstream of the promoter. An Nco I fragment that contained the *TRP1* gene was inserted at the Nco I site of the *URA3* gene, and the resulting plasmid was termed pHR307a. The plasmid $p(lexO)^2$ is pHR307a with two *lexA* operator sequences [R. Brent and M. Ptashne, *Nature* **312**, 612 (1984)] inserted at the Eco RI sites. The plasmid $p(B1)^3$ was constructed by adding two copies of the B1 fragment to the B1 reporter plasmid.
10. Yeast bearing the appropriate activator plasmid were transformed [H. Ito, Y. Fukada, K. Murata, A. Kimura,

J. Bacteriol. **153**, 163 (1983)] with a reporter library and plated on minimal medium [F. Sherman, G. R. Fink, J. B. Hicks, *Laboratory Course Manual for Methods in Yeast Genetics* (Cold Spring Harbor Laboratory, Cold Spring Harbor, NY, 1986)] lacking uracil and tryptophan at a density of ~300 yeast per 10-cm dish. After 3 days of growth at 30°C, the yeast were replica-plated to medium lacking histidine (containing both uracil and tryptophan). After 6 days of growth, the yeast were replica- plated to medium lacking histidine and with or without 1% 5-FOA (PCR, Gainesville, FL). Colonies that grew on 5-FOA–lacking but not 5-FOA–containing plates were picked and the plasmids recovered into bacteria for analysis [C. S. Hofman and F. Winston, *Gene* **57**, 267 (1987)].

11. J. D. Boeke, F. LaCroute, G. R. Fink, *Mol. Gen. Genet.* **197**, 345 (1984).
12. A. R. Oliphant, C. J. Brandl, K. Struhl, *Mol. Cell. Biol.* **9**, 2944 (1989).
13. D. E. Hill, I. A. Hope, J. P. Macke, K. Struhl, *Science* **234**, 451 (1986).
14. We constructed the genomic reporter library by partially digesting rat genomic DNA with Mbo I to different extents, pooling the digests, and purifying the 75- to 500-bp fragments by elution from gels. These fragments were cloned into the Bam HI sites of the mp7 polylinker of pHR307a and a library of 30,000 transformants was obtained. Random oligonucleotides were created by mutually primed synthesis [A. R. Oliphant, A. L. Nussbaum, K. Struhl, *Gene* **44**, 177 (1986)], such that each oligonucleotide contained 23 degenerate nucleotides with Eco RI–Sac I ends. These oligonucleotides were cloned into a modified pHR307a, and a library of 10,000 transformants was obtained. Random oligonucleotide clones contained an average of three oligonucleotides per clone. Approximately 1% of the oligonucleotide library and 10% of the genomic library were His^+ in the absence of plasmid-expressed activator.
15. K. Struhl, *Cell* **50**, 841 (1987).
16. R. Brent and M. Ptashne, *ibid.* **43**, 729 (1985).
17. M. Ptashne, *Nature* **335**, 683 (1988); P. J. Mitchell and R. Tjian, *Science* **245**, 371 (1989).
18. R. Brent and M. Ptashne, *Proc. Natl. Acad. Sci. U.S.A.* **78**, 4204 (1981).
19. The plasmid pLG was derived from p1027 (*16*) as follows: The Xho I site in the *URA3-CEN3-ARS1* vector pRS316 was destroyed by fusing it to the adjacent Sal I site. The 5-kb Bam HI cassette of p1027, which contains the *lexA-GAL4* coding sequence linked to the constitutive *ADC1* promoter, was then transferred into the altered pRS316 vector. We constructed pLBG by inserting an NGFI-B zinc finger–encoding fragment into the Xho I site of the LG coding region. This fragment, obtained from a polymerase chain reaction performed with the NGFI-B cDNA and with primers with Xho I ends, extends from nucleotide 899 to nucleotide 1165 of the NGFI-B cDNA (*2*).
20. K. Hamada *et al.*, *Proc. Natl. Acad. Sci. U.S.A.* **86**, 8289 (1989).
21. M. J. Shea, D. L. King, M. J. Conboy, B. D. Mariani, F. C. Kafatos, *Genes Dev.* **4**, 1128 (1990).
22. L. Wang *et al.*, *Nature* **340**, 163 (1989); Y. P. Hwung, D. T. Crowe, L. H. Wang, S. Y. Tsai, M. J. Tsai, *Mol. Cell. Biol.* **8**, 2070 (1988).
23. D. D. Chaplin, L. J. Galbraith, J. G. Seidman, P. C. White, K. L. Parker, *Proc. Natl. Acad. Sci. U.S.A.* **83**, 9601 (1986); K. I. Morohashi, K. Sogawa, T. Omura, Y. Fujii-Kuriyama, *J. Biochem. (Tokyo)* **101**, 879 (1987); S. Shibahara *et al.*, *EMBO J.* **2**, 775 (1983).
24. Lipid binding protein genes that contain an NBRE include the genes for the intestinal [D. A. Sweetser *et al.*, *J. Biol. Chem.* **262**, 16060 (1987)] and adipose [J. S. Cook *et al.*, *Proc. Natl. Acad. Sci. U.S.A.* **85**, 2949 (1988)] fatty acid binding proteins, apolipoproteins CIII [A. A. Protter *et al.*, *DNA* **3**, 449 (1984)] and B-100 [B. D. Blackhart *et al.*, *J. Biol. Chem.* **261**, 15364 (1986)], cellular retinol binding protein II [L. A. Demmer *et al.*, *ibid.* **262**, 2458 (1987)], human serum prealbumin [H. Sasaki, N. Yosioka, Y. Takagi, Y. Sakaki, *Gene* **37**, 191 (1985)], and acyl-coenzyme A oxidase [T. Osumi, N. Ishii, S. Miyazawa, T. Hashimoto, *J. Biol. Chem.* **262**, 8138 (1987)].
25. B. A. Evans and R. I. Richards, *EMBO J.* **4**, 133 (1985); C. M. Crowder and J. P. Merlie, *Mol. Cell. Biol.* **8**, 5257 (1988); R. A. DePinho *et al.*, *Proc. Natl. Acad. Sci. U.S.A.* **83**, 1827 (1986).
26. The Pro36-Luc vector contains the firefly luciferase coding region downstream of a minimal prolactin promoter [S. Adler, M. L. Waterman, X. He, M. G. Rosenfeld, *Cell* **52**, 685 (1988)]. The B1 fragment and the B1a oligonucleotide were inserted into the Bam HI site upstream of the promoter. Plasmid $p(B1a)^8$-Luc contains eight copies of the B1a oligonucleotide repeated in tandem. The mammalian expression plasmid pCMV has a polylinker downstream of the cytomegalovirus (CMV) promoter. We made pCMV–(NGFI-B) by cutting an NGFI-B cDNA–containing Bluescript (Stratagene) plasmid with Bam HI (which cuts in the polylinker just upstream of the NGFI-B initiation codon) and Mlu I (which cuts the NGFI-B cDNA at nucleotide 1918, just downstream of the termination codon) and then by ligating the product to pCMV cut with Bgl II and Mlu I. We made pCMV–(NGFI-Bt) by cutting a second NGFI-B cDNA–containing Bluescript clone with Aat II [which cuts the NGFI-B cDNA at nucleotide 1353 (amino acid 380, ~80 residues downstream of the zinc fingers)], fusing the product to the downstream Bam HI site in the polylinker, and adding a translation terminator at the Xba I site further downstream. The product was excised from Bluescript with Not I and Nco I (nucleotide 211 of the NGFI-B cDNA), Hind III linkers were added, and the fragment was ligated into the Hind III site of pCMV.
27. COS-7 cells were grown in Dulbecco's modified Eagles's medium supplemented with 10% fetal bovine serum. Cells were plated 24 hours before transfection at a density of 700,000 cells per 10-cm dish. The cells were transfected by calcium phosphate precipitation [C. Chen and H. Okayama, *Mol. Cell. Biol.* **7**, 2745 (1987)] with a total of 10 μg of plasmid DNA per plate (5 μg of activator plasmid, 5 μg of reporter plasmid). Three days after transfection, the cells were washed twice with ice-cold phosphate-buffered saline and lysed by incubation in 0.7 ml of 50 mM tris-MES (pH 7.8), 1 mM dithiothreitol, and 1% Triton X-100 for 5 min at room temperature. The lysate was cleared of cellular debris by centrifugation. Luciferase assays were performed on 50 μl of cell lysate as described [J. R. de Wet, K. V. Wood, M. DeLuca, D. R. Helinski, S. Subrami, *Mol. Cell. Biol.* **7**, 725 (1987)] with a Monolight 2010 luminometer (Analytical Bioluminescence Laboratory, San Diego, CA). All values represent the results of at least two different experiments, each performed with different preparation of DNA.
28. P. J. Godowski, S. Rusconi, R. Miesfield, K. R. Yamamoto, *Nature* **325**, 365 (1987); S. M. Hollenberg, V. Giguere, P. Segui, R. M. Evans, *Cell* **49**, 39 (1987); H. Gronemeyer *et al.*, *EMBO J.* **6**, 3985 (1988); V. Kumar *et al.*, *Cell* **51**, 941 (1987).
29. K. W. Kinzler and B. Vogelstein, *Mol. Cell. Biol.* **10**, 634 (1990); L. Sompayrac and K. J. Danna, *Proc. Natl. Acad. Sci. U.S.A.* **87**, 3274 (1990); T. K. Blackwell and H. Weintraub, *Science* **250**, 1104 (1990).
30. To screen one mammalian genome equivalent of DNA (3×10^9 bp) for target genes, one would need to plate at least 6×10^6 reporter-containing yeast colonies with a modal insert size of 500 bp, a prohibitive number. Yeast (~10^7 bp) and *Drosophila* (~10^8 bp) genomes could be screened completely with ~10^4 and ~10^5 clones, respectively.
31. The probability (P) of obtaining the observed or a larger number of 7-bp GCN4 sites from each library was calculated with the Poisson distribution, $P(x) = e^{-m}(m^x/x!)$; where x is the number of sites obtained, n is the total number of UAS nucleotides selected, and $m = 2n/4^7$.
32. V. Zimarino and C. Wu, *Nature* **327**, 727 (1987).
33. The *GCN4* expression plasmid p164 was obtained from A. Hinnebusch, plasmid p1027 from R. Brent, the Pro36-Luc vector from S. Adler, and the pCMV expression plasmid from M. Roth. We thank T. Ley, S. Adler, and J. Majors for critical reading of the manuscript. Supported by PHS grants NS01018 from the National Institute of Neurological and Communicative Diseases and Stroke and by PO1 CA49712 from the National Cancer Institute and by grant RG1779B2 from the Multiple Sclerosis Foundation.

8 January 1991; accepted 22 March 1991

Proximate Constraints on the Evolution of Egg Size, Number, and Total Clutch Mass in Lizards

BARRY SINERVO AND PAUL LICHT

Proximate constraints on egg size, number, and total clutch mass in side-blotched lizards were examined by experimentally reducing average clutch size from 4.6 eggs to one, two, and three eggs. Eggs from experimentally altered clutches were larger than those from controls, reflecting the trade-off between egg size and number. Moreover, the increased frequency of females with oviducally bound eggs or eggs that burst at oviposition suggests that egg size in clutches with very few eggs are at a functional upper size limit. These proximate constraints may also limit evolution of egg size in another group of lizards (*Anolis*) that only produces one-egged clutches.

IMPLICIT IN CONSIDERATIONS OF many traits that covary consistently among phylogenetically related groups of organisms is that these traits are in some fashion constrained and this constraint reflects an underlying mechanistic trade-off among these traits. Indeed, the notion of a trade-off among suites of traits making up the organismal life history has become a paradigm of evolutionary biology (*1*). For example, the presumed trade-off between clutch or litter size and offspring size is a fundamental aspect of life history theory (*2*) and is a pervasive pattern among vertebrates (*3*). Given functional and energetic limitations on total clutch or litter mass, it seems intuitively obvious that a female producing larger offspring must produce fewer offspring than a female producing a smaller offspring. Moreover, at one end of this continuum, a second type of constraint may impose further limits on adaptive evolution—the diameter of the pelvic girdle has been suggested to be a functional limit to the maximum offspring size that is possible

Department of Integrative Biology, University of California, Berkeley, CA 94720.